CFD code comparison, verification and validation for a FOWT semi-submersible floater (OC4 Phase II)

Pranav Chandramouli[1], Manuel Rentschler[2,*], Axelle Viré[1], Guilherme Vaz[2,3] and Rodolfo T. Gonçalves[4]

[1] Wind Energy Section, Faculty of Aerospace Engineering, TU Delft

[2] WavEC Offshore Renewables, Portugal

[3] Department of Civil, Maritime and Environmental Engineering, University of Southampton, UK

[4] OSPL - Ocean Space Planning Laboratory, The University of Tokyo, Japan

[*] Corresponding author: Manuel Rentschler, manuel.rentschler@wavec.org

ABSTRACT

With the advancement of high-performance computation capabilities in recent years, high-fidelity modelling tools such as Computational Fluid Dynamics (CFD) are becoming increasingly popular in the offshore renewable sector. In order to justify the credibility of the numerical simulations, thorough verification and validation is essential. In this work, decay tests for a freely floating cylinder and a linearly moored floating offshore wind turbine (FOWT) model of the OC4 (Offshore Code Comparison Collaboration Continuation) phase II semi-submersible platform are simulated. Two different viscous flow CFD codes are used: OpenFOAM (open-source), and ReFRESCO (community based open-usage). Their results are compared against each other and with water tank experiments. The data from experimental and numerical tests is made freely available on the web hosting platform GitHub [1], inviting other researchers to join the code comparison and build a reference validation case for floating offshore wind turbines.

Keywords: Computational Fluid Dynamics (CFD), Floating Offshore Wind Turbine (FOWT), OC4, Decay test, Verification & Validation.

1 INTRODUCTION

Computational Fluid Dynamics (CFD) has become an integral part in the design process for numerous fields such as in the design of aircrafts, automobiles, submarines, and oil platforms, to name a few. Recently, with the advances in the field of floating offshore wind energy, CFD has taken a major role in advancing the design for floating offshore wind turbines (FOWT). The application of CFD in the field is diverse from analysing platform hydrodynamics, to turbine aerodynamics along with wind farm control and layout optimisation. However, the underlying physics associated with FOWT is complex, having to account for the interaction between the platform and the turbine along with the effect of waves and wind. This also presents a significant challenge for experimental methods. Novel methods have been developed involving scale-model testing of FOWT. However, the downscaling is difficult as there is a mismatch between the aerodynamic scaling laws dictated by the Reynolds number and the hydrodynamic scaling laws based on the Froude number. New methods such as the hardware-in-loop (HIL) experimental techniques were developed wherein the aerodynamics and the hydrodynamics are either modelled numerically or physically reproduced. Two broader groups within this are the ocean basin HIL method where the aerodynamics is modelled and the hydrodynamics is reproduced with the hardware, and vice-versa with the wind tunnel HIL technique.

[1] `https://github.com/WavEC-Offshore-Renewables/tokyo-wavec-fowt`

The current state of the art experimental methods, while still improving, still require numerical inputs to emulate real-life conditions. This involves a strong reliance on methods such as CFD which can provide, based on the experimental method used, either the aerodynamic forces on the rotor or the hydrodynamic forces on the platform. For performing CFD analyses, there are numerous codes that are commerically (ANSYS Fluent, Star CCM, Fine/Marine), and openly (OpenFOAM, Incompact3D, Fluidity) available. These include comprehensive programs capable of simulating a wide variety of flows (OpenFOAM, ANSYS Fluent), and more niche codes focused on specific numerical methods and/or particular flow physics (ReFRESCO, Incompact3d). Given the wide variety of choices, a comparative study is crucial to understand the strengths and shortcoming of different codes/solvers. In this work, we will focus on two CFD solvers, namely the open-source generalist code OpenFOAM, and the community-based maritime-focused code ReFRESCO. The case-study is the decay analysis of the OC4 semi-submersible platform designed by Robertson et al. (2014) and experimentally studied by Gonçalves et al. (2020). The numerical results will be compared with the experimental data. A preliminary validation study of the codes is also performed with the decay simulation of a 3D circular cylinder in heave and pitch and compared with the data from Palm et al. (2016). This flow was also used as a validation tool by Rivera-Arreba et al. (2019) to further study the OC5 semi-submersible platform.
The layout of the article is as follows. Section 2 summarises the underlying numerical methods of the two CFD solvers and the numerical set-up for the two case-studies. In section 3, the results and discussions are presented for the two test cases. Finally, section 4 summarises the major outcomes of the research and recommendations for future work.

2 NUMERICAL METHODS

In the following section, the numerical methods and the underlying theory of the CFD simulations are described. After a quick overview of the governing equations, the two CFD codes are described highlighting the differences across the solvers. This is followed by a numerical description of the two case-studies analysed in this work.
The governing equations are the incompressible, multi-phase Navier-Stokes equations with the conservation of mass,

$$\frac{\partial \rho}{\partial t} + \frac{\partial (\rho u_i)}{\partial x_i} = 0, \tag{1}$$

and the conservation of momentum,

$$\frac{\partial (\rho u_i)}{\partial t} + \frac{\partial (\rho u_i u_j)}{\partial x_j} = -\frac{\partial p}{\partial x_i} + \frac{\partial}{\partial x_j}\left(\mu\left(\frac{\partial u_i}{\partial x_j} + \frac{\partial u_j}{\partial x_i}\right)\right) + \rho f_i. \tag{2}$$

A Reynolds averaging is applied for turbulent flows resulting in the Reynolds-Averaged Navier-Stokes (RANS) equations, i.e.

$$\frac{\partial (\rho \overline{u}_i)}{\partial x_i} = 0, \tag{3}$$

$$\frac{\partial (\rho \overline{u}_i)}{\partial t} + \frac{\partial}{\partial x_j}\left(\rho \overline{u}_i \overline{u}_j + \rho \overline{u_i' u_j'}\right) = -\frac{\partial \overline{p}}{\partial x_i} + \frac{\partial}{\partial x_j}\left(\mu\left(\frac{\partial \overline{u}_i}{\partial x_j} + \frac{\partial \overline{u}_j}{\partial x_i}\right)\right) + \rho \overline{f}_i. \tag{4}$$

The contributions of the turbulent small scales $\rho\overline{u_i' u_j'}$, also called Reynolds stresses, need to be additionally modelled to close the system of equations. In this work, the k-ω SST model developed by Menter et al. (2003) is adopted across all turbulent simulations.
The two solvers used in this work are ReFRESCO[2] (v2.6.0) and OpenFOAM (v1606)[3]. ReFRESCO is a community-based, open-usage, finite-volume based CFD solver focusing on maritime applications. It solves the unsteady, incompressible, Navier-Stokes equations incorporating user-chosen turbulence models (Vaz et al., 2009). A cell-centered collocated approach is used for variables in strong-conservation form. OpenFOAM is a free to use, open-source, finite-volume based CFD solver. The

[2] https://www.marin.nl/facilities-and-tools/software-sales/refresco
[3] https://www.openfoam.com/

Table 1. Solvers

Equations	ReFRESCO	OpenFOAM
Mass		
Solver	BCGS	PBiCG
Preconditioner	Block-Jacobi	DILU
Momentum		
Solver	BCGS	PBiCG
Preconditioner	Jacobi	DILU
Free surface		
Solver	BCGS	PBiCG
Preconditioner	Jacobi	DILU
Pressure coupling		
Solver	FreSCo	PIMPLE
Turbulence		
Solver	GMRES	Smooth

solver is capable of handling a wide variety of fluid simulations including multi-phase turbulent flows which are the focus of this work.
For all simulations, the implicit first-order Euler time-advancement scheme is used in both solvers. The gradient is approximated using a second order Gauss Linear scheme while the turbulence is modelled using the k-ω SST model. The pressure-velocity coupling is handling using the SIMPLE algorithm in ReFRESCO (Klaij and Vuik, 2013) while it is combined with the PISO algorithm in OpenFOAM to give the PIMPLE methodology. An attempt is made across the two codes and case-studies to maintain similarity in the solvers employed.
The free-surface is modelled using the well-known volume-of-fluid (VOF) method (Klaij et al., 2018) in both solvers which is capable of handling mesh-motion and adaptive re-meshing. The rigid-body mechanics is captured by solving the structural equations of motion in all six degrees of freedom (DoF). The rigid-body solver accounts for external constraints such as hydrodynamics forces, restraints, and moorings (Burmester et al., 2020). The motion of the body is handled with a deforming grid algorithm in ReFRESCO (de Boer et al., 2007) and a laplacian equation solver for motion displacement in OpenFOAM. Wave absorption zones are implemented to damp waves origination from body motion. ReFRESCO has inherent capability to handle these zones (Rapuc et al., 2018) while the additional WAVES2FOAM toolbox (Jacobsen and Fredsøe, 2012; Jensen and Christensen, 2014) needs to be implemented in OpenFOAM to handle wave absorption. The list of solvers and preconditioners implemented are tabulated in Tab. 1.

3 RESULTS AND DISCUSSIONS

This sections presents the two case-studies analysed in this work. The first sub-section focuses on the validation case-study of a free floating 3D cylinder experimentally studied in Palm et al. (2016) and used for validation purposes by Rivera-Arreba et al. (2019). The second sub-section focuses on the decay study of the OC4 platform designed by Robertson et al. (2014) and experimentally studied by Gonçalves et al. (2020). Each sub-sections is divided into two parts with the former describing the numerical set-up and the latter presenting and analysing the results.

3.1 Free Floating Cylinder

3.1.1 Set-up

The freely floating 3D cylinder is placed in a rectangular domain measuring $x = 15m$, $y = 5m$, and $z = 1.8m$ with the cylinder placed at the origin $(0, 0, 0)$. The inlet is at $x = -6m$ and the outlet at $x = 9m$. The cylinder is in the middle of the vertical domain and the sides of the domain are at

Table 2. Transport properties for air and water for the free floating cylinder decay tests

Fluid	Transport Model	Kinematic Viscosity (ν) $[m^2/s]$	Density (ρ) $[kg/m^3]$
Water	Newtonian	1e-6	1000
Air	Newtonian	1.5e-5	1.2

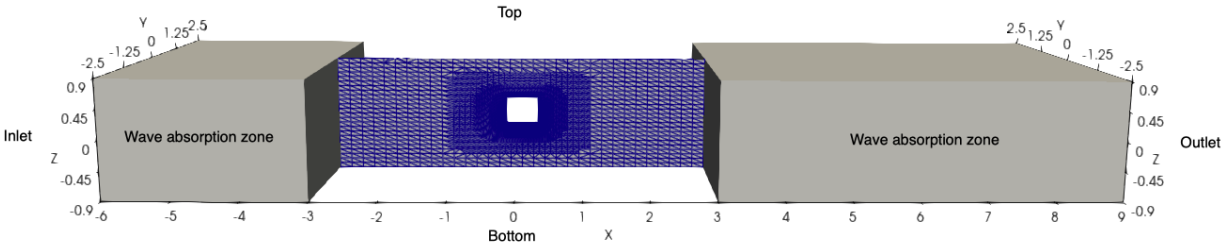

Figure 1. 3D free floating cylinder domain and boundary conditions. The wave absorption zones are indicated as grey boxes. The cylinder is placed at origin $(0, 0, 0)$

$y = \pm 2.5$. Two wave absorption zones are defined at the inlet and outlet extending up to $x = -3m$ in the former and beginning at $x = 3m$ in the latter.

The mesh is created using the commercial software HEXPRESS[4] with refinement zones defined around the cylinder with three refinement steps in the horizontal direction and an additional step in the vertical directions aimed at better resolving the water surface. The resultant mesh is a fully unstructured hexahedral mesh with $5.11 * 10^5$ cells for a resolution of 15 cells per diameter (cpd) of the cylinder. ReFRESCO has the ability to deform an initial mesh wherein the cylinder can be moved from its equilibrium position to the initial displacement for the decay test using the deforming grid algorithm. However, OpenFOAM is currently lacking this functionality and requires the mesh to already account for the displacement of the body. This results in an initial mesh that varies slightly for the two solvers, however, this was seen to have little to no effect on the results.

The cylinder diameter is $D = 0.515m$ with a height $H = 0.4m$. It has a total mass of $m = 35.85kg$ with an inertia of $I_{yy} = 0.9kg \cdot m^2$ resulting in a draft of $0.172m$ and a KG of $0.0758m$. For the pitch decay test, the KG and moment of inertia values are modified to $KG = 0.0818m$ and $I_{yy} = 0.95kg \cdot m^2$ as per the calibration study performed by Rivera-Arreba et al. (2019). The boundary conditions are tabulated in Tab. 3. As only heave and pitch decay tests are performed, the lateral y domain is reduced by half with a symmetry condition imposed at $y = 0$. No turbulence model is employed as the flow is laminar with damped waves. The transport properties for the two phases are given in Tab. 2.

[4] `https://www.numeca.com/product/omnis-hexpress`

Table 3. Free floating cylinder case-study boundary conditions

Boundary	ReFRESCO	OpenFOAM
Back	Slip wall	Slip wall
Bottom	Slip wall	Slip wall
Mirror	Symmetry	Symmetry
Atmosphere	$p = 0$	totalPressure
Inlet	$\mathbf{u} = (1\text{e-}6; 0; 0)\,\mathrm{ms}^{-1}$	zeroGradient
Outlet	$\mathbf{u} = (1\text{e-}6; 0; 0)\,\mathrm{ms}^{-1}$	zeroGradient
Cylinder	No-slip wall	No-slip wall

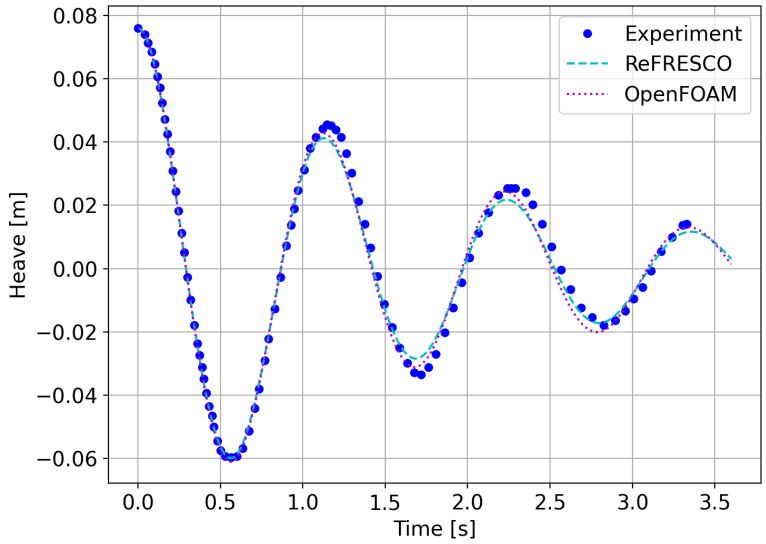

(a)

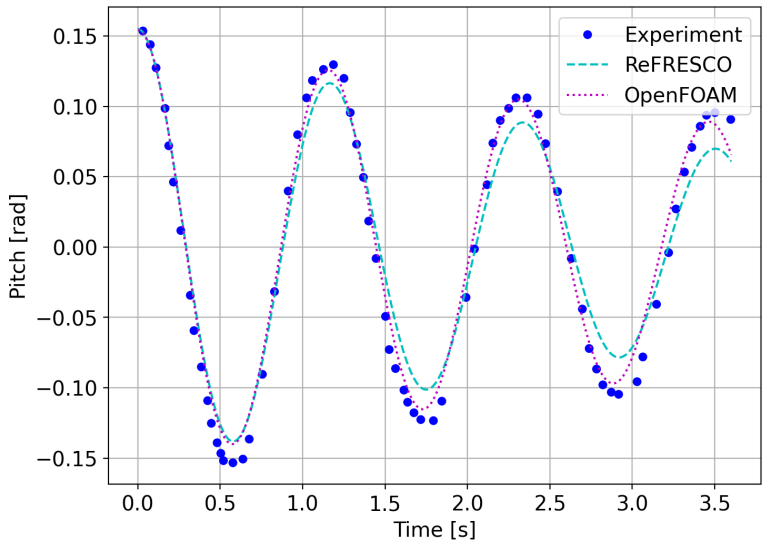

(b)

Figure 2. Free floating cylinder decay motion in heave (top) and pitch (bottom) from OpenFOAM and ReFRESCO compared with experimental data of Palm et al. (2016).

3.1.2 Decay Study

Heave and pitch decay tests are performed with the free floating cylinder. The initial heave off-set is set at $0.076m$ and the initial pitch rotation is set to $8.88°$ around the centre of gravity as per the right hand rule. The simulations are run in 3DoF (free motion in heave, pitch and surge) and for a duration of 3 decay periods with a time step of $\Delta t = 0.002s$. The resultant heave and pitch decay motion are plotted in Fig. 2.

For heave decay, OpenFOAM and ReFRESCO predict accurately both the natural period and the damping. Both solutions are slightly over-damped with ReFRESCO having the strongest damping. The values of the natural period and linear damping coefficient in heave are tabulated in Tab. 4. An error of 0.08% and 0.6% is observed in the prediction of the natural period for OpenFOAM and ReFRESCO respectively. For linear damping, an error of 0.38% and 8.5% is noted indicative of the strong damping imposed by ReFRESCO.

In pitch decay, a larger deviation in motion can be observed especially in the results of ReFRESCO which once again has a larger damping as compared to the experiment than OpenFOAM. ReFRESCO

Table 4. Cylinder natural period and linear damping coefficient in heave and pitch decay.

	ReFRESCO		OpenFOAM		Experiment	
	T_n [s]	θ [-]	T_n [s]	θ [-]	T_n [s]	θ [-]
Heave	1.119	-0.560	1.113	-0.518	1.112	-0.516
Pitch	1.168	-0.232	1.154	-0.159	1.170	-0.148

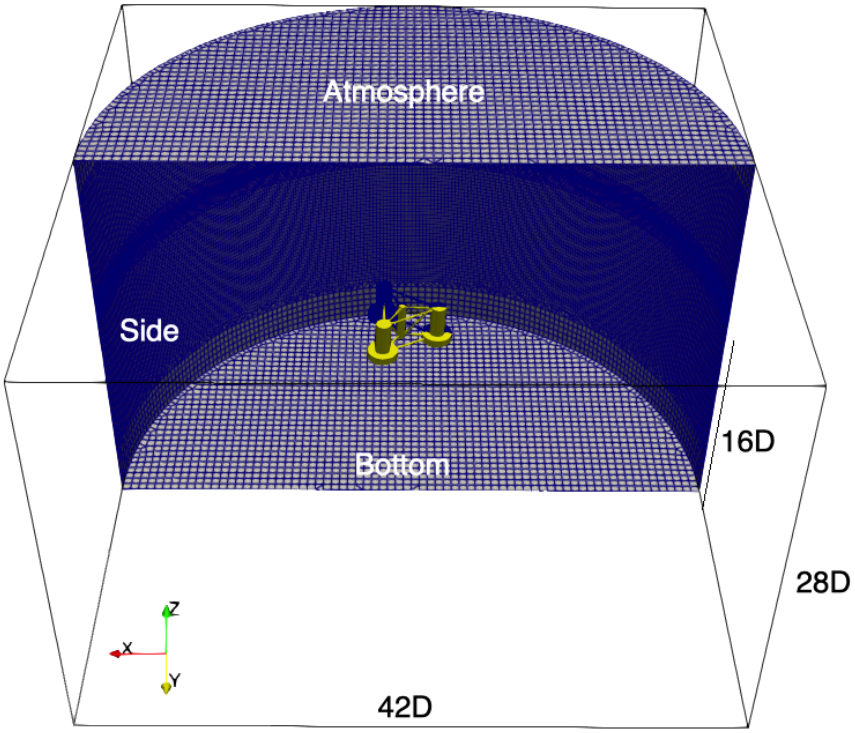

Figure 3. OC4 semi-submersible model domain and boundary conditions.

does predict the natural period with a lower error of 0.34% compared to OpenFOAM with an error of 1.3%. A study performed by Rivera-Arreba et al. (2019) suggests that the measured dynamic properties of the cylinder body from Palm et al. (2016) includes some experimental error and that numerical simulations are highly susceptible to changes in the structural properties. The errors observed in the prediction of pitch decay motion could be attributed to this numerical dependency. A linear damping error of 7.4% and 56.7% is observed for OpenFOAM and ReFRESCO respectively. Although the damping error is notable for ReFRESCO, this is a result not only of the higher damping in ReFRESCO but also a function of the material properties of the cylinder and errors in their estimation.

3.2 OC4 Semi-Submersible Floater

3.2.1 Set-up

The OC4 semisubmersible platform was designed by Robertson et al. (2014) for phase II: hydrodynamic studies for the Offshore Code Comparison Collaboration Continuation (OC4) project. The original design for the semisubmersible was developed for the DeepCwind project and further optimised in the OC4 project work. This platform, in a scaled-down version (1:72.73), was experimentally studied by Gonçalves et al. (2020) in a towing-tank. In this work, the scaled-down model is numerically studied with OpenFOAM and ReFRESCO and compared with the experimental results of Gonçalves et al. (2020).

Table 5. OC4 semisubmersible boundary conditions

Boundary	ReFRESCO	OpenFOAM
Side	Sommerfeld1	zeroGradient
Bottom	$p = 0$	slip
Atmosphere	$p = 0$	totalPressure
Platform	No-slip wall	No-slip wall

Table 6. Semi-submersible dimensions and structural properties.

Upper column Diameter [m]	Height [m]	Draft [m]	Mass [kg]	KG [m]	I_{**} [kgm^2]
0.165	0.44	0.275	36.7	0.134	4

The semisubmersible platform is placed in a cylindrical domain (see Fig. 3) with a height of 28D, and a diameter of 42D, where D is the diameter of the upper column of the scaled-down semisubmersible measuring $D = 0.165m$. The origin $(0, 0, 0)$ is on the static free-surface at a height of 16D from the bottom and 12D from the top. The boundary conditions are tabulated in Tab. 5. The scaled-down submersible has a mass of $36.7kg$ with an inertia of $I_{xx} = I_{yy} = I_{zz} = 4kg \cdot m^2$. The height is measured at $0.44m$ with an upper column diameter D of $0.165m$ and a draft of $0.275m$ and a KG of $0.134m$. These properties are concisely given in Tab. 6.
The mesh is created using HEXPRESS with a background mesh resolution of 14 cells per upper column diameter in the near field around the semi-submersible. This resolution is similar to the 15 cpd of the free floating cylinder. Additional refinement is performed on the free surface to capture the waves created due to body motion. The boundary layer is captured with a fine viscous layer mesh conforming to $y+ < 1$. Refinement is also carried out on the surface of the platform focusing on sharp edges and intersections. The resultant mesh contains ~ 11 million hexahedral cells.
Four mooring lines are attached to the platform. In equilibrium conditions, two lines are attached to the anchor and the platform in the $x = 0$ plane (referred to as front and back springs) and two lines in the $y = 0$ plane (referred to as left and right springs). The mooring lines are modelled as linear springs in the solvers. The attachment location on the body and anchor points along with the spring parameters are tabulated in Tab. 7.
The $k - \omega$ SST turbulence model, developed by Menter et al. (2003), is activated for modelling the turbulent small scales. The transport properties for the two phases (air and water) are identical to the free floating cylinder experiment given in Tab. 2.

3.2.2 Decay Study

Surge and sway decay tests are performed on the semi-submersible platform with the two solvers. An initial off-set of one upper-column diameter ($D = 0.165m$) is enforced on the platform. For OpenFOAM, the off-set was accounted for in the meshing process while in ReFRESCO this was done with the deforming algorithm within the solver. Each simulation is run for a total of three periods. In

Table 7. Semi-submersible mooring line parameters under equilibrium conditions.

Springs	Anchor	Attachment Point	Stiffness $[N/m]$	Damping $[Ns/m]$	Rest Length $[m]$
Front	$(2.4, 0, 0.375)$	$(0.49, 0, 0.17)$	7.4556	0	0.8
Back	$(-2.4, 0, 0.375)$	$(-0.49, 0, 0.17)$	7.4556	0	0.8
Left	$(0, -1.59, 0.375)$	$(0, -0.49, 0.17)$	9.4176	0	0.425
Right	$(0, 1.59, 0.375)$	$(0, 0.49, 0.17)$	9.4176	0	0.425

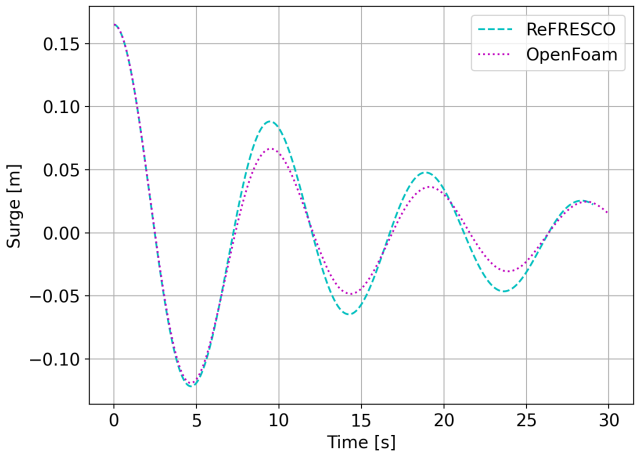

(a)

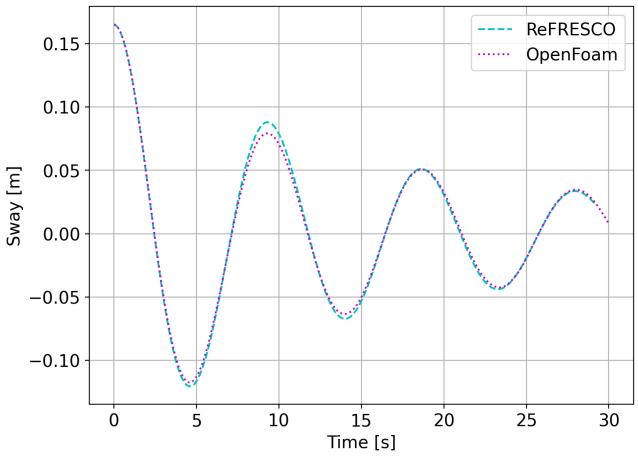

(b)

Figure 4. OC4 semi-submersible decay motion in surge (top) and sway (bottom) from OpenFOAM and ReFRESCO.

ReFRESCO, a fixed time step of $0.001s$ is chosen. In OpenFOAM, an adjustable time-step is chosen with an initial value of $0.0025s$ and a maximum Courant number limitation of $Co < 2$ and an interface based Courant number limitation of $Co_\alpha < 0.25$.

The resultant motion is matched with the experimental results of Gonçalves et al. (2020) through comparison of the natural periods and damping coefficients. At first, only 1 DoF calculations are performed for each decay test focusing on the primary motion that is to be captured. The resultant decay motion for surge and sway are plotted in Fig. 4 for OpenFOAM and ReFRESCO.

The results indicate that OpenFOAM predicts higher damping of the motion as compared to ReFRESCO for the semi-submersible. This is contrary to the results that were observed with the free-floating cylinder. One reason for this difference could be the restriction of the motion to one DoF - this limits interaction across the DoFs and could lead to the differing results. The natural periods are in agreement across the two solvers for both decay studies. These values are compared with the experiment in Tab. 8 along with the linear damping coefficients.

For surge, an error of 1.5%, and 71.8% for the natural period and linear damping coefficient is seen for OpenFOAM as compared to 0.5% and 59.0% for ReFRESCO. For sway, the values are 2.8% and 44.7% for OpenFOAM and for ReFRESCO, 3% and 47.4%. These results suggest that numerically the natural period can be accurately captured by existing models while the damping of the motion is still inaccurate. This inaccuracy could be due to a multitude of factors: the restriction of motion to a single degree of freedom in the simulations, errors in the platform material properties (as was seen for the floating cylinder), experimental errors in measurement, numerical errors due to model selection

Table 8. Semi-submersible natural period and linear damping coefficient in heave and pitch decay

	ReFRESCO		OpenFOAM		Experiment	
	T_n [s]	θ [-]	T_n [s]	θ [-]	T_n [s]	θ [-]
Surge	9.45	0.062	9.55	0.067	9.4	0.039
Sway	9.32	0.056	9.33	0.055	9.6	0.038

Table 9. Cylinder natural period and linear damping coefficient in Heave and Pitch decay

	OpenFOAM (1DoF)		OpenFOAM (6DoF)		Experiment	
	T_n [s]	θ [-]	T_n [s]	θ [-]	T_n [s]	θ [-]
Surge	9.55	0.067	9.79	0.052	9.4	0.039
Sway	9.33	0.055	9.59	0.054	9.6	0.038

(turbulence model, discretisation method, etc.). It is to be noted that the methodology for calculating the linear damping coefficients for the experiments were not provided. Thus, significant error in the linear damping could be attributed to differing methodologies for estimating the coefficient.
To analyse the effect of degrees of freedom, additional simulations have been carried out with OpenFOAM with 6DoF (i.e. no imposed restriction on body motion). The decay motion between the 1DoF and 6DoF simulations for surge and sway are compared in Fig. 5.
A deviation can be observed in the results for both natural period and damping in surge and in the natural period for sway. It is interesting to note that damping remains similar for sway for both simulations. The resultant natural period and damping coefficients are given in Tab. 9. A contrasting trend is seen in the natural period with a better prediction for sway (0.1% error) and a worsening prediction for surge (4.1% error). For linear damping, the increase in the DoF results in an improved coefficient prediction for both surge (33.3% error as compared to 71.8% error for 1DoF) and sway (42.1% error as compared to 44.7% error for 1DoF).

4 CONCLUSIONS

In this work, a comparative study of two CFD solvers, OpenFOAM and ReFRESCO, has been performed for the hydrodynamic decay study of a semi-submersible platform used in floating offshore wind energy. The solvers are validated with a preliminary study on a free floating 3D cylinder in heave and pitch decay. ReFRESCO predicted higher damping of the decay motion in both degrees of freedom as compared to OpenFOAM. ReFRESCO accurately predicted the natural period for both tests while OpenFOAM had a mixed performance with an accurate heave natural period but a larger error for pitch natural period.
The study on the OC4 semi-submersible platform was performed with a scaled down (1:72.73) model of the original design. The scaled down model was studied experimentally by Gonçalves et al. (2020) and the numerical results were compared with these experimental measurements. Surge and sway decay tests were performed with both solvers with restriction body motion (1DoF). ReFRESCO performed marginally better than OpenFOAM across all results. Lower damping was observed with ReFRESCO as compared to OpenFOAM - this was contrary to the observations on the floating cylinder case study. Additional 6DoF studies with OpenFOAM suggested that linear damping is better predicted when no restrictions are imposed on body motion. This dependency will be further studied in future works for both OpenFOAM and ReFRESCO.
The study suggests that existing numerical codes are capable of predicting the natural period for free/forced decay motion with high accuracy. However, the damping of the motion tends to be over-predicted leading to highly damped oscillations as compared to experimental results. Restricting body motion leads to further increase in motion damping. An interesting future avenue of research could be the characterisation of numerical and experimental inaccuracies associated with the damping

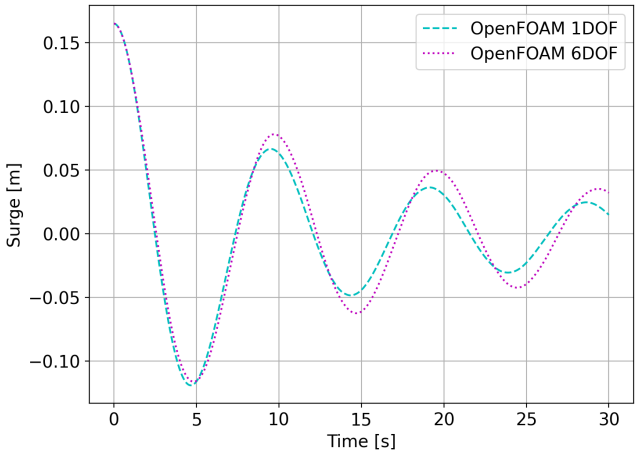

(a)

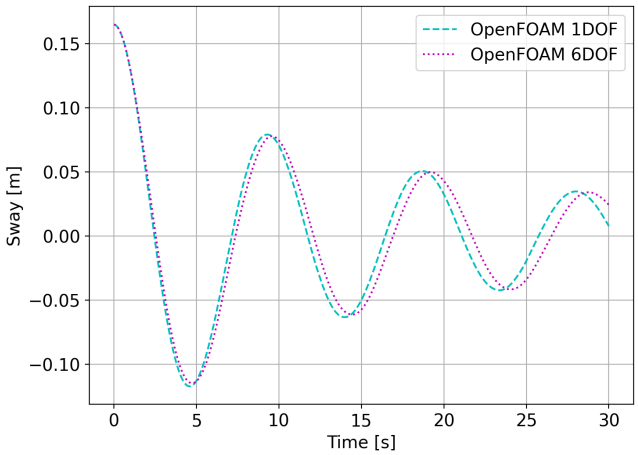

(b)

Figure 5. OC4 semi-submersible decay motion in surge (top) and sway (bottom) from OpenFOAM in 1DoF and in 6DoF.

coefficients to identify the sources of maximum error.

ACKNOWLEDGEMENTS

The authors acknowledge the use of the IRIDIS High Performance Computing Facility, the Dutch national e-infrastructure with the support of SURF Cooperative, and associated support services at the University of Southampton. They would also like to acknowledge the support by the European Union's Horizon 2020 research and innovation programme (project TWIND, grant agreement no. 857631). AV is also grateful for the support by the European Union's Horizon 2020 research and innovation programme via the STEP4WIND project (grant agreement no. 860737).

REFERENCES

Burmester, S., Vaz, G., el Moctar, O., Gueydon, S., Koop, A., Wang, Y., and Chen, H. C. (2020). High-Fidelity Modelling of Floating Offshore Wind Turbine Platforms. volume Volume 9: Ocean Renewable Energy of *International Conference on Offshore Mechanics and Arctic Engineering*.

de Boer, A., van der Schoot, M. S., and Bijl, H. (2007). Mesh deformation based on radial basis function interpolation. *Computers & Structures*, 85(11):784–795.

Gonçalves, R. T., Chame, M. E. F., Silva, L. S. P., Koop, A., Hirabayashi, S., and Suzuki, H. (2020). Experimental Flow-Induced Motions of a FOWT Semi-Submersible Type (OC4 Phase II Floater). *Journal of Offshore Mechanics and Arctic Engineering*, 143(1).

Jacobsen, N. G. Fuhrman, D. R. and Fredsøe, J. (2012). A Wave Generation Toolbox for the Open-Source CFD Library: OpenFoam. *International Journal for Numerical Methods in Fluids*, 70(9):1073–1088.

Jensen, B. Jacobsen, N. G. and Christensen, E. D. (2014). Investigations on the porous media equations and resistance coefficients for coastal structures. *Coastal Engineering*, 84:56–72.

Klaij, C., Hoekstra, M., and Vaz, G. (2018). Design, analysis and verification of a volume-of-fluid model with interface-capturing scheme. *Computers & Fluids*, 170:324–340.

Klaij, C. M. and Vuik, C. (2013). SIMPLE-type preconditioners for cell-centered, collocated finite volume discretization of incompressible Reynolds-Averaged Navier-Stokes equations. *International Journal for Numerical Methods in Fluids*, 71(7):830–849.

Menter, F. R., Kuntz, M., and Langtry, R. (2003). Ten Years of Industrial Experience with the SST Turbulence Model. *Turbulence, Heat and Mass Transfer*, 4:625–632.

Palm, J., Eskilsson, C., Paredes, G. M., and Bergdahl, L. (2016). Coupled mooring analysis for floating wave energy converters using CFD: Formulation and validation. *International Journal of Marine Energy*, 16:83–99.

Rapuc, S., Crepier, P., Jaouen, F., Bunnik, T., and Regnier, P. (2018). Towards guidelines for consistent wave propagation in CFD simulations. 19th International Conference on Ship & Maritime Research (NAV2018).

Rivera-Arreba, I., Bruinsma, N., Bachynski, E. E., Viré, A., Paulsen, B. T., and Jacobsen, N. G. (2019). Modeling of a Semisubmersible Floating Offshore Wind Platform in Severe Waves. *Journal of Offshore Mechanics and Arctic Engineering*, 141(6).

Robertson, A., Jonkman, J., Masciola, M., Song, H., Goupee, A., Coulling, A., and Luan, C. (2014). Definition of the Semisubmersible Floating System for Phase II of OC4. Technical report, NREL.

Vaz, G., Jaouen, F., and Hoekstra, M. (2009). Free-Surface Viscous Flow Computations: Validation of URANS Code FreSCo. volume Volume 5: Polar and Arctic Sciences and Technology; CFD and VIV of *International Conference on Offshore Mechanics and Arctic Engineering*, pages 425–437.